Check for
updates

Numerical analysis of impact ionization in HOT HgCdTe avalanche photodiodes

M. Kopytko[1] · E. Gomółka[1] · K. Jóźwikowski[1]

Abstract

Semiconductor avalanche photodiodes enable individual photons to be detected when the incident flux of light is very low. This is possible thanks to the use of the avalanche multiplication phenomenon. Consequently, the obtained gain of photocurrent is from a few to several million times. The avalanche multiplication effect in semiconductors is determined by the generation rate caused by impact ionization. This paper describes the results of research aimed at investigation of the impact ionization mechanism in HgCdTe photodiodes operating at 230 K and in the medium-wave infrared range. Numerical analyses were used for the study using a computer program in which the modeling and consideration of all the possible generation and recombination mechanisms were included.

1 Introduction

Among many types of infrared (IR) detectors, some of them enable (for example) individual photons to be detected when the incident flux of light is very low. For many years, photomultiplier tubes (PMTs) have been used to detect very weak signals. Despite the high sensitivity and high gain amounting of at several million, they have a significant deficiency, such as a low quantum efficiency, incorrect operation in the presence of magnetic fields, have a large size and not persistent design.

Semiconductor devices, particularly avalanche photodiodes (APDs), are alternatives to photomultipliers. Avalanche photodiodes can detect electromagnetic radiation of extremely low intensity. By applying a high reverse bias voltage, APDs show an internal current gain effect due to impact ionization (avalanche effect). Under the influence of a high electric field, the electrons/holes in the depletion region of an APDs are accelerated and gradually acquire sufficient kinetic energy to impact ionize other electrons/holes leading to the junction break-down. It results in current gain of even several million times

✉ M. Kopytko
malgorzata.kopytko@wat.edu.pl

[1]   Institute of Applied Physics, Military University of Technology, 2 Kaliskiego St., 00-908 Warsaw, Poland

(depending on the applied voltage—the higher the reverse voltage, the higher the gain). APDs with the highest operating gain allow detection of single photons. Due to the ability of very weak signals detection in a short time intervals, APDs are widely used in laser rangefinders, optical radars, long-range free space or optic telecommunication and ultra-sensitive spectroscopy.

Present APDs are as sensitive as photomultipliers, and at the same time are much smaller and more convenient to use. The highest performance of the mid-wavelength infrared (MWIR) and long-wave infrared (LWIR) HgCdTe APDs has been obtained at low temperatures (77 K) with high gain at low reverse bias, low excess noise factor, and low dark currents (Reine et al. 2007; Beck et al. 2011; Kinch et al. 2004). High operating temperature (HOT) conditions (IR detectors operated close to room temperature or thermoelectrically cooled) of MWIR APDs can be achieved in architecture so-called separate absorption and multiplication heterostructure APDs (SAM-APDs), so far implemented in III–V technology (Wang et al. 2014; Ren et al. 2016) and in HgCdTe in the near-infrared (NIR) radiation (1–2 μm) (Lyon et al. 1999). CEA-LETI has presented stable multiplication gains in homojunction HgCdTe APDs with cutoff wavelengths down to 2.8 μm and operating temperatures up to 300 K (Rothman et al. 2012) and first experimental results of planar heterostructure HgCdTe APDs with high gain and low dark current at 200 K (Rothman et al. 2009).

In this paper we present some designs of HgCdTe APDs proposed for HOT conditions—detectors operated using 2-stage thermoelectrical coolers (230 K). We use numerical simulations to investigate the impact ionization process in HgCdTe photodiodes to determine the ability of the avalanche multiplication.

2 Impact ionization model

The number of electron–hole pairs generated by a carrier per unit distance travelled is called the ionization coefficient of charge carrier. The ratio of ionization coefficients of hole and electron is defined as $k = \alpha_h/\alpha_e$, which is often used to characterize excess noise. In some semiconductors electrons ionize more efficiently than holes (Si, GaAsSb, InGaAs, for which $\alpha_e > \alpha_h$), while in others the reverse is true (Ge, GaAs, where $\alpha_h > \alpha_e$). In $Hg_{1-x}Cd_xTe$, the electron to hole impact ionization ratio is dependent on the Cd composition (Singh et al. 2011). The hole ionization is favorable for the NIR HgCdTe detectors ($0.5 < x < 0.7$). In this case, the energy required for the excitation of an electron from the valence band to the conduction is equal to the energy of spin–orbit splitting holes. The electron ionization is favorable for the MWIR and LWIR ($x < 0.5$) which based on one-band transitions. Due to conservation of energy and momentum, a threshold energy, E_{th}, prerequisite has to be satisfied by the primary carrier. This energy has to be greater than the band gap, E_g, as the carrier also experiences non-ionizing collision processes such as phonon scattering, which involves carriers gaining energy, losing energy or exchanging momentum.

When the electric field in a semiconductor is increased above a certain value, the carriers gain enough energy (greater than the band gap) so that they can excite electron–hole pairs by impact ionization. In the local-field theory, the equation which governs the electron and hole impact ionization current is equal (McIntyre 1999):

$$G_{ION} = \frac{1}{q}\alpha_e j_n + \frac{1}{q}\alpha_h j_p, \tag{1}$$

where q is the elementary charge, α_e and α_h are functions only of the electric field. Experimentally, it has been found that the electron and hole ionization coefficients, in the limit of low field ε, can be represented by the expressions:

$$\alpha_e = a_e \exp\left(-b_e\big/\varepsilon^{m_e}\right), \tag{2}$$

$$\alpha_h = a_h \exp\left(-b_h\big/\varepsilon^{m_h}\right), \tag{3}$$

where m_e and m_h are close to unity at least at low field. In our calculations the values of coefficients $a_e = 3 \times 10^5$ cm^{-1} and $b_e = 1.5 \times 10^5$ cm^{-1} have been assumed after (Kinch 2007).

Current density is usually expressed as functions of quasi-Fermi levels:

$$\vec{j}_n = q\mu_e n\nabla\Phi_n, \tag{4}$$

$$\vec{j}_p = q\mu_h p\nabla\Phi_p, \tag{5}$$

where μ denotes the mobility and Φ is the quasi-Fermi level. The indices n and p denote electron and hole, respectively.

In our model, as in other works (Qiu et al. 2015; Li et al. 2018; Cheng et al. 2019), the impact ionization is expressed as the net generation rate, G_{ION}. In this way we can introduce it directly to transport equations (Roosbroeck 1950; Kurata 1982) with other generation-recombination (GR) mechanisms including influence of thermal mechanisms (Shockley–Read–Hall (SRH), Auger, Radiative) as well as tunneling mechanisms due to band-to-band tunneling (BTB) and trap-assisted tunneling (TAT). The detailed description of our model can be found in previous papers (Jóźwikowski et al. 2010a,b). All key parameters associated with particular GR mechanisms assumed in the simulation are listed in Table 1.

Table 1 Parameters associated with GR mechanisms taken in modelling

Trap concentration, N_T (cm^{-3})	5×10^{13}
Trap ionisation energy, E_T	$3/4 E_g$
Trap capture coefficient, c_n, c_p (cm^3 s^{-1})	1.5×10^{-7}, 3×10^{-9}
Dislocations density, G_{GIS} (cm^{-2})	10^6
Dislocations ionisation energy, E_T	$0.32 E_g$
Dislocations capture coefficient, c_n, c_p (cm^3 s^{-1})	3×10^{-7}, 6×10^{-8}
Coefficients a_e and b_e in Eq. (2) (cm^{-1})	3×10^5, 1.5×10^5
Ratio of ionization coefficients for electrons and holes, k	0.05
Overlap matrix $F_1 F_2$	0.3

3 Device design

First photodiode (N^+–p–P^+ type) is a classical $Hg_{1-x}Cd_xTe$ design built on the basis of two heterojunctions (Fig. 1a). The Cd molar composition in the active area of $x_{Abs}=0.36$ was chosen to obtain a long-term sensitivity limit ($\lambda_{cut\text{-}off}$) of about 3.5 µm at 230 K. It was assumed that the absorber is a p-type layer doped with arsenic at the level of 5×10^{15} cm^{-3}. Contacts are wide-bandgap layers with the Cd molar composition of 0.45: bottom contact layer is n-type doped with iodine at the level of 2×10^{17} cm^{-3} and cap contact layer is p-type doped with arsenic at the level of 5×10^{17} cm^{-3}. At the absorber and contact layers interfaces we assumed the x-graded regions created by interdiffusion processes during HgCdTe growth.

Second photodiode (N^+–n–p–P^+ type) contains an additional avalanche region (multiplication region) introduced between the bottom contact layer and the absorber (Fig. 1b). In the proposed structure, the key item is to obtain the lowest level of doping in the avalanche multiplication area in order to reduce unfavorable tunneling processes. We assumed the n-type doping in this region at the level of 5×10^{14} cm^{-3}. In the first approach, the Cd molar composition of the avalanche region was assumed the same as for the absorber ($x_{Aval}=x_{Abs}=0.36$) and the thickness of this region has been set as 1 µm. In the second approach, the molar composition and thickness of the avalanche region were changed to investigate the net generation rate due to impact ionization in this region. All device simulation parameters are summarized in Table 2.

4 Results and discussion

Figure 2 presents a spatial distribution of the electric field in detectors operating at a zero and a reverse bias voltage of −2 V and −4 V. Calculations were performed for the detector temperature of 230 K. In the N^+–p–P^+ detector, the electric field is deposited near the
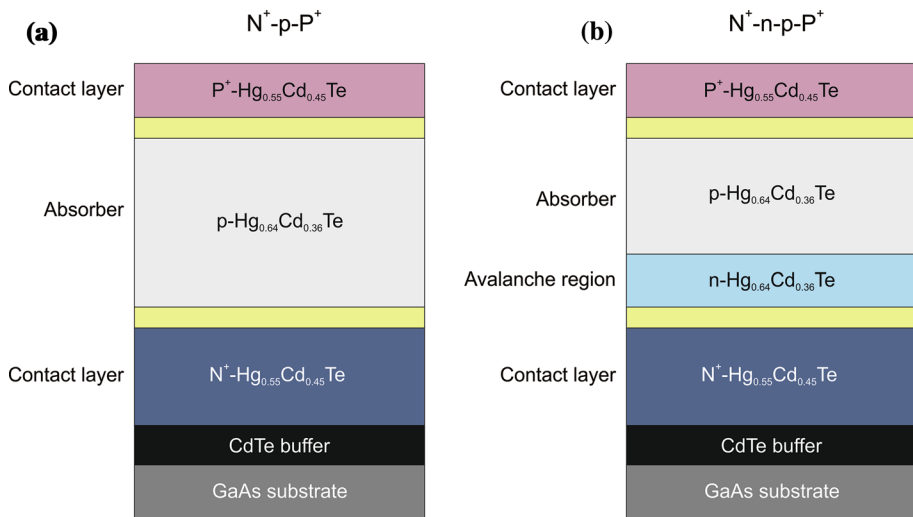

(a) N^+-p-P^+

Contact layer	P^+-$Hg_{0.55}Cd_{0.45}Te$
Absorber	p-$Hg_{0.64}Cd_{0.36}Te$
Contact layer	N^+-$Hg_{0.55}Cd_{0.45}Te$
	CdTe buffer
	GaAs substrate

(b) N^+-n-p-P^+

Contact layer	P^+-$Hg_{0.55}Cd_{0.45}Te$
Absorber	p-$Hg_{0.64}Cd_{0.36}Te$
Avalanche region	n-$Hg_{0.64}Cd_{0.36}Te$
Contact layer	N^+-$Hg_{0.55}Cd_{0.45}Te$
	CdTe buffer
	GaAs substrate

Fig. 1 Cross-section scheme of a HgCdTe photodiodes with a N^+–p–P^+ (**a**) and N^+–n–p–P^+ (**b**) configuration

Table 2 N^+–n–p–P^+ type device parameters taken in modelling

	Bottom contact (N^+)	Avalanche region (n)	Absorber (p)	Cap contact (P^+)
Thickness (µm)	2	1	2	1
Doping (cm^{-3})	2×10^{17}	5×10^{14}	5×10^{15}	5×10^{17}
Composition	0.45	0.36	0.36	0.45
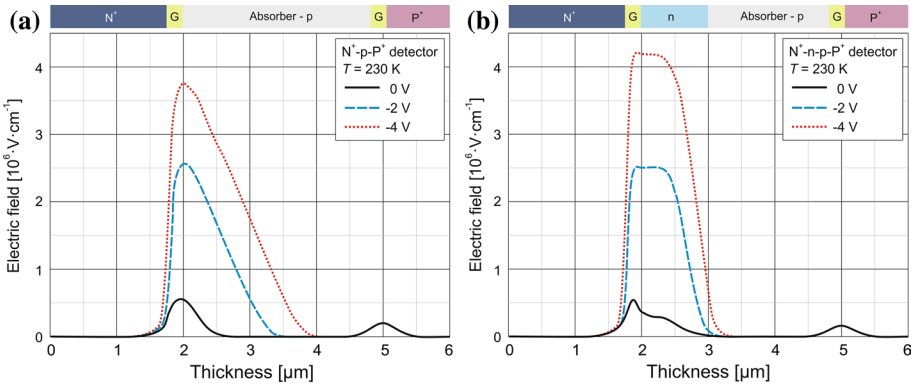
Fig. 2 Calculated distribution of the electric field in the HgCdTe photodiode in N^+–p–P^+ (**a**) and N^+–n–p–P^+ (**b**) configuration

absorber and the bottom contact junction and extends into the absorber with the increasing bias voltage. In the case of the N^+–n–p–P^+ detector, the electric field reaches a higher value and is located mainly in the avalanche region. The active region remains the electric field free. The value and the distribution of the electric field will have an influence on the rate of the impact ionization.

The dependencies of the current density and the maximum net generation rate associated with the impact ionization as a function of the bias voltage calculated for N^+–p–P^+ and N^+–n–p–P^+ detectors operating at 230 K are shown in Figs. 3 and 4 respectively. The current associated with the avalanche multiplication increases for voltage above −2.5 V. For the bias voltage of −5 V it is about an order of magnitude larger in the N^+–n–p–P^+ detector than in the N^+–p–P^+ detector. This is the result of a greater (by an order of magnitude) the net impact ionization rate.

Next, the influence of the molar composition and thickness of the avalanche region on the impact ionization were analyzed. Figure 5 show the current–voltage characteristics calculated for N^+–n–p–P^+ detector with the assumption of different molar composition (the molar composition was increased compared to the absorber molar composition by 0.01) and thickness (the thickness was changed from 1 up to 2 µm) of the avalanche region. The densities of dark currents decrease both with the increase of the molar composition and thickness of the avalanche region. However, the change of the thickness has a greater effect on the dark current values. It can be seen that when the thickness of the avalanche region is twice thicker, a much higher bias voltage (almost twice as large) should be applied in order to achieve the same value of the current associated with the impact ionization (see Fig. 5b).

Fig. 3 Dark current density plotted as a function of the reverse bias voltage for the HgCdTe photodiode in N^+–p–P^+ and N^+–n–p–P^+ configuration
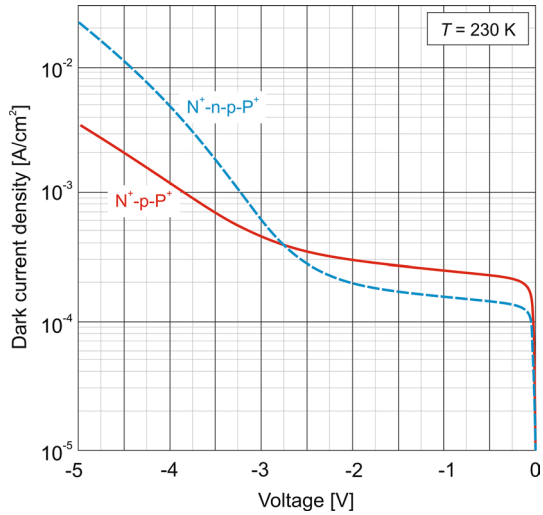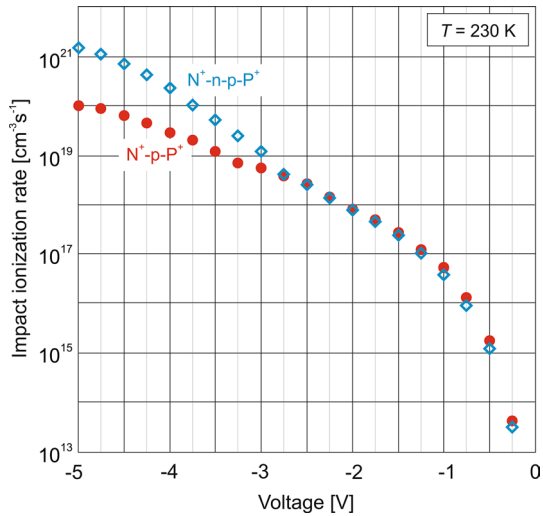

Fig. 4 Net generation rate due to impact ionization plotted as a function of the reverse bias voltage for the HgCdTe photodiode in N^+–p–P^+ and N^+–n–p–P^+ configuration.

The extension of the energy gap in the multiplication area also influences the net generation rate associated with the impact ionization—it decreases with increasing the energy gap of this area (Fig. 6a). Also the thickness increasing of the avalanche region significantly influences the net generation rate associated with the impact ionization. At a bias of −5 V it decreases by almost two orders of magnitude in the area of twice the thickness (Fig. 6b).
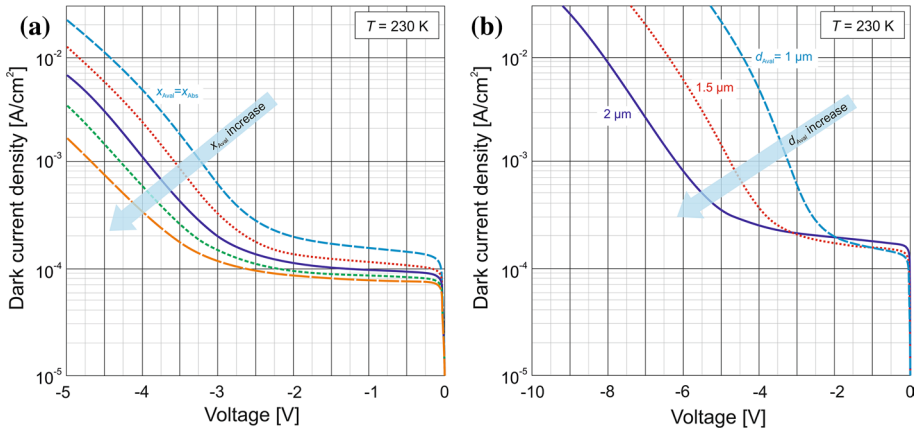
Fig. 5 Dark current density in the N^+–n–p–P^+HgCdTe photodiode plotted as a function of the Cd molar composition (**a**) and thickness (**b**) of the avalanche region
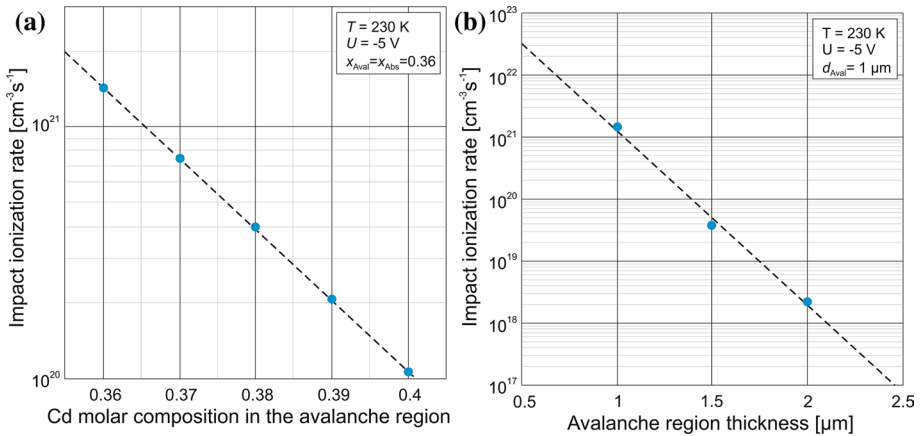

Fig. 6 Net generation rate due to impact ionization in the N^+–n–p–P^+HgCdTe photodiode plotted as a function of the Cd molar composition (**a**) and thickness (**b**) of the avalanche region

5 Conclusions

APDs operating in the wavelength range up to 14 μm can be constructed on the basis of HgCdTe. However, they must be cooled to a liquid nitrogen temperature to reduce the thermal processes of excitation of charge carriers. This paper presents the results of the theoretical analysis of the impact ionization to determine the possibility of designing HgCdTe APDs cooled using thermoelectric coolers (operating at 230 K). Numerical analyzes were performed for a classical HgCdTe photodiode built on the basis of two heterojunctions (N^+–p–P^+ configuration) and photodiode with an additional avalanche multiplication region (N^+–n–p–P^+ configuration).

Results show that at 230 K avalanche multiplication can be achieved in a HgCdTe photodiode without a separate area for the carrier multiplication. However, much better results can be obtained when the carrier multiplication region and active region are separated. By reverse biasing the N^+–n–p–P^+ detector with a high voltage, the electric field is mainly distributed in the carrier multiplication region, while the N^+–p–P^+ detector, the electric field extends into the absorber area. Higher electric field in the multiplication region results in increased net generation rate associated with the impact ionization.

The influence of the molar composition and thickness of the avalanche region on the impact ionization were also analyzed for the N^+–n–p–P^+ detector. The net generation rate due to the impact ionization decreases both with the increase of the molar composition and thickness of the avalanche region and the change of the thickness has a greater effect on the impact ionization. To obtain the same value of the impact ionization rate almost twice as large bias voltage should be applied when the thickness of the avalanche region is twice thicker.

References

Beck, J.D., Wan, C.F., Kinch, M.A., Robinson, J.E.: MWIR HgCdTe avalanche photodiodes. Proc. SPIE. **4454**, 188–197 (2011)

Cheng, Y., Chen, L., Guo, H., Lin, C., He, L.: Improved local field model for HgCdTe electron avalanche photodiode. Infrared Phys. Technol. **101**, 156–161 (2019)

de Lyon, T.J., Baumgratz, B., Chapman, G., Gordon, E., Hunter, A.T., Jack, M., Jensen, J.E., Johnson, W., Johs, B., Kosai, K., Larsen, W., Olson, G.L., Sen, M., Walker, B., Wu, O.K.: MBE growth of HgCdTe avalanche photodiode structures for low-noise 1.55 μm photodetection. J. Cryst. Growth **201**(202), 980–984 (1999)

Jóźwikowski, K., Kopytko, M., Rogalski, A., Jóźwikowska, A.: Enhanced numerical analysis of current-voltage characteristics of long wavelength infrared n-on-p HgCdTe photodiodes. J. Appl. Phys. **108**, 074519–074529 (2010a)

Jóźwikowski, K., Kopytko, M., Rogalski, A.: Enhanced numerical analysis of current-voltage characteristics of long wavelength infrared p-on-n HgCdTe photodiodes. Bull. Pol. Acad. Sci. **58**, 523–533 (2010b)

Kinch, M.A.: Fundamentals of Infrared Detectors Materials, pp. 110–112. SPIE Press, Bellingham (2007)

Kinch, M.A., Beck, J.D., Wan, C.F., Ma, F., Campbell, J.: HgCdTe electron avalanche photodiodes. J. Electron. Mater. **33**, 630–639 (2004)

Kurata, M.: Numerical Analysis of Semiconductor Devices. Lexington Books DC Heath, Lexington (1982)

Li, Q., He, J., Hu, W.: Influencing sources for dark current transport and avalanche mechanisms in planar and mesa HgCdTe pin electron-avalanche photodiodes. IEEE Trans. Electron Devices **65**(2), 572–576 (2018)

McIntyre, R.J.: A new look at impact ionization—Part I: a theory of gain, noise, breakdown probability and frequency response. IEEE Trans. Electron Devices **46**, 1623–1631 (1999)

Qiu, W.C., Hu, W.-D., Chen, L., Lin, C., Cheng, X.-A., Chen, X.-S., Lu, W.: Dark current transport and avalanche mechanism in hgcdte electron-avalanche photodiodes. IEEE Trans. Electron Devices **62**(6), 1926–1931 (2015)

Reine, M.B., Marciniec, J.W., Wong, K.K., Parodos, T., Mullarkey, J.D., Lamarre, P.A., et al.: HgCdTe MWIR back illuminated electron initiated avalanche photodiode arrays. J. Electron. Mater. **36**, 1059–1067 (2007)

Ren, M., Maddox, S.J., Woodson, M.E., Chen, Y., Bank, S.R., Campbell, J.C.: AlInAsSb separate absorption, charge, and multiplication avalanche photodiodes. Appl. Phys. Lett. **108**, 191108 (2016)

Rothman, J., Baier, N., Ballet, P., Mollard, L., Fournier, M., Gout, J.S., Chamonal, J.P.: High-operating temperature HgCdTe avalanche photodiodes. J. Electron. Mater. **38**, 1707–1716 (2009)

Rothman, J., Mollard, L., Bosson, S., Vojetta, G., Foubert, K., Gatti, S., Bonnouvrier, G., Salveti, F., Kerlain, A., Pacaud, O.: Short-wave infrared HgCdTe avalanche photodiodes. J. Electron. Mater. **41**, 2928–2936 (2012)

Singh, A., Srivastav, V., Pal, R.: HgCdTe avalanche photodiodes: A review. Opti. Laser Technol. **43**, 1358–1370 (2011)

Van Roosbroeck, W.: Theory of the electrons and holes in germanium and other semiconductors. Bell Syst. Tech. J. **29**, 560–607 (1950)

Wang, X., Hu, W., Pan, M., Hou, L., Xie, W., Xu, J., Li, X., Chen, X., Lu, W.: Study of gain and photoresponse characteristics for back-illuminated separate absorption and multiplication GaN avalanche photodiodes. J. Appl. Phys. **115**, 013103 (2014)